Noise Induced Phase Transition in a Two-dimensional Coupled Map Lattice

Valery I. Sbitnev*
Department of Condensed State Research,
B. P. Konstantinov Petersburg Nuclear Physics Institute,
Russian Academy of Science,
Gatchina, Leningrad district, 188350, Russia

The phase transition with respect to the intensity of a δ-correlated noise source has been studied in a coupled map lattice that simulates the excitability of field-type neural tissues [7]. The entropy of lattice states *versus* this control parameter undergoes a qualitative change at the phase transition point. Its behavior is linear on one side of this point and it transforms to a cubic-root form on the other side. An enormously increasing susceptibility to external perturbation in the vicinity of the phase transition point leads to an observed existence of stochastic resonance in this region. Complexity induced by the external subthreshold periodic signal reaches a maximum at the phase transition point.

1. Introduction

Complexity, emerging from system pattern formations, has attracted the close attention of researchers for a long time [3, 5, 6, 15, 29, 34]. Such investigations are closely related to studies of phase transition phenomena [1, 16, 24]. Fluctuations that grow enormously in the vicinity of a phase transition point become the sources of new phase nucleating centers. Intrinsic system noise is a powerful mutagenic factor providing reproduction of complexity [19–22, 25, 26]. If noise intensity is a control parameter then an emergence of complex patterns can be expected in the vicinity of phase transitions with respect to this parameter [10].

In this paper phase transition in a two-dimensional coupled map lattice with a δ-correlated additive noise source is studied. Lattice parameters are specified so that a point attractor $\varphi_0 = 0$ exists in the absence of noise (Figure 1). There is a threshold φ_{thr} that separates the basin of the attractor from the rest of the phase space, where chaotic bursts emerge. Noise sometimes pushes the system out from the attractor basin. Such an excursion to the burst region induces traveling waves which can propagate for long distances if the coupling strength of the lattice sites is large enough.

*Electronic mail address: sbitnev@hep486.pnpi.spb.ru.

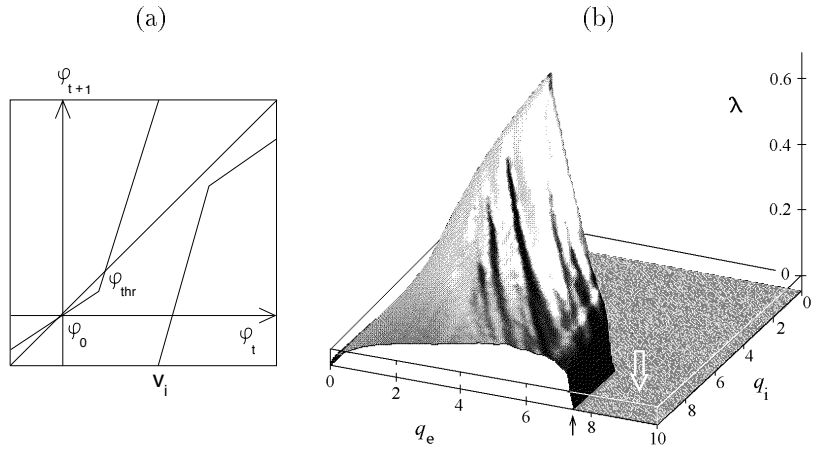

Figure 1. Piecewise-linear map. (a) The map depicted at parameters chosen from a region pointed to by the white arrow in the right graph. (b) The Lyapunov exponent of the piecewise-linear map, parameters q_i and q_e are explained in the text. The black arrow points to the Pomeau–Manneville bifurcation boundary, that is, the boundary where two fixed points φ_0 and φ_{thr} (see the left graph) are annihilated [28].

As known from phase transition physics, system susceptibility to external perturbation increases dramatically as the control parameter nears the phase transition point. Let the perturbation be a periodic subthreshold signal $A^0 \cos[\Omega \cdot t]$ applied to the system being studied. Such a statement of the problem has culminated in the investigations of stochastic resonance (SR) [32], that are widely presented in the literature (for a review see [12]). Noise enhanced spatiotemporal pattern formation representing, in fact, spatiotemporal SR has been recently studied as well [22, 25, 26]. In the present work this problem is studied with respect to phenomena that occur at nonequilibrium phase transitions.

This paper is organized as follows. The two-dimensional coupled map lattice (CML) is described in section 2, as well as properties of the single-site map (Figure 1). In section 3 the noise induced phase transition in two-dimensional CML is discussed. It is found that the Shannon entropy undergoes a change in behavior as the noise intensity passes through the phase transition point. Section 4 deals with SR that causes entropy excess in the vicinity of the phase transition point. This excess is assumed to be an indicator of complexity [1, 5, 24] reproduced by the external subthreshold input. In section 5 we summarize the results and cast a glance at information processing of nervous systems through these findings.

2. Two-dimensional coupled map lattice

The two-dimensional CML under consideration in this paper is

$$\begin{aligned}\varphi^{t+1}_{n,m} &= (1-\gamma)(\varphi^{t}_{n,m} + \zeta\Delta^{t}_{n,m}) \\ &\quad + q_e S[\varphi^{t}_{n,m} + \zeta\Delta^{t}_{n,m} - v_e] - q_i\theta[\varphi^{t}_{n,m} - v_i] \\ &\quad + \xi^{t}_{n,m} + A^{0}_{n,m}\cos[\Omega\cdot t]. \end{aligned} \tag{1}$$

Here the sigmoid function $S[x]$ is represented by its piecewise-linear version [4, 6, 35]

$$S[x] = \frac{1}{2} + \frac{1}{4}\left(\left|\frac{x}{2}+1\right| - \left|\frac{x}{2}-1\right|\right), \tag{2}$$

and $\theta[x]$ is the Heaviside step function. Thresholds v_e and v_i in these functions are expressed *via* the parameters q_e and q_i in the following manner [7, 30]:

$$v_s = \ln[q_s + \exp[-q_s]], \qquad s = e, i. \tag{3}$$

Due to this restriction [11], a number of the system parameters can be reduced.

The diffusion term $\Delta^{t}_{n,m}$ in equation (1) has the form

$$\Delta^{t}_{n,m} = \varrho^{t}_{n,m} - \varphi^{t}_{n,m}. \tag{4}$$

Here

$$\varrho^{t}_{n,m} = \frac{\sum_{j,k}\varpi_{n+j,m+k}\cdot\varphi^{t}_{n+j,m+k}}{\sum_{j,k}\varpi_{n+j,m+k}}, \tag{5}$$

$j, k = -1, 0, 1$, and $\varpi_{n+j,m+k}$ is a projection operator

$$\begin{aligned}\varpi_{n+j,m+k} &= \delta_{|j|+|k|,1}\cdot\theta[n+j]\times\theta[m+k] \\ &\quad \times\theta[N+1-(n+j)]\times\theta[N+1-(m+k)], \end{aligned} \tag{6}$$

providing free boundary conditions [31]. Here $\delta_{|j|+|k|,1}$ is the Kronecker delta function.

The external periodic signal $A^{0}_{n,m}\cos[\Omega\cdot t]$ is applied to the central part of the lattice of size $N^2 = 64\times 64$:

$$A^{0}_{n,m} = \begin{cases} A^0, & n,m \subset [24;\ 40] \\ 0, & n,m \not\subset [24;\ 40]. \end{cases} \tag{7}$$

The noise values $\xi^{t}_{n,m}$ at every lattice site (n, m) and at every time $t = 1, 2, \ldots$ are generated by the Box–Muller algorithm [23]

$$\xi = \sigma(-2\ln[r_1])^{1/2}\cos[2\pi r_2] \tag{8}$$

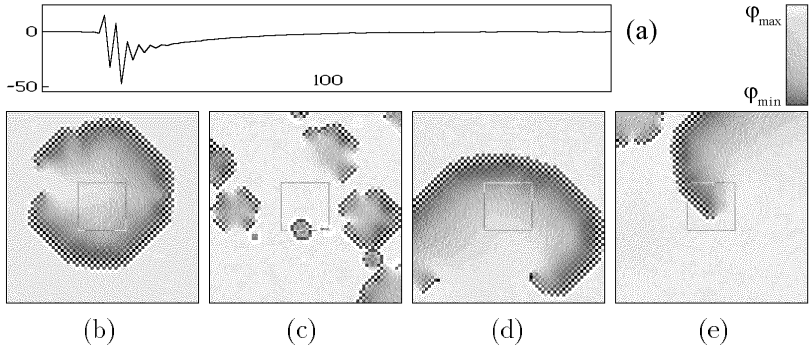

Figure 2. (a) Record of $\varphi^t_{n,m}$ showing a burst together with a suppressed tail. Snapshots of traveling waves emerged under a small periodic signal ($A^0 = 0.012$, $T_\Omega = 2\pi/\Omega = 120$) and at different noise amplitudes σ: (b) $\ln[\sigma] = -2.3$ (near onset of SR), target waves emerge predominantly within the driven (central) area and propagate outside; (c) $\ln[\sigma] = -1.8$ (large noise amplitude), target waves are emerging everywhere in the lattice; (d) clockwise spiral wave, $\ln[\sigma] = -2.1$; (e) counterclockwise spiral wave, $\ln[\sigma] = -1.6$. The 16×16 squares drawn in the central parts of the 64×64 lattice space show areas wherein the periodic signal from equation (7) is applied with $q_i = 20$, $q_e = 10$, $\gamma = 0.07$, and $\zeta = 0.8$.

from two uniformly distributed random numbers (on the unit interval) r_1 and r_2. For this reason, the internal noise $\xi^t_{n,m}$ is the gaussian δ-correlated noise with intensity σ^2 [9]

$$\langle \xi^t_{n,m} \rangle = 0, \qquad \langle \xi^t_{n,m} \xi^\tau_{k,l} \rangle = \sigma^2 \cdot \delta_{n,k} \delta_{m,l} \delta_{t,\tau}. \tag{9}$$

The system parameters q_i, q_e, and $\gamma \ll 1$ are set to $q_i = 20$, $q_e = 10$, and $\gamma = 0.07$, so that the steady state $\varphi^t_{n,m} = 0$, $\forall n, m, t$ occurs in the absence of the external signal and noise. In essence, $\varphi^t_{n,m} = 0$ is a point attractor of the system separated from a region of bursting activity by the threshold (see Figure 1)

$$\varphi_{\text{thr}} = \frac{\nu_e - 2}{1 - 4\gamma/q_e}. \tag{10}$$

Given $q_e = 10$ and $\gamma = 0.07$ we estimate $\varphi_{\text{thr}} \approx 0.311$. Obviously, the amplitude of an input signal A^0 should be small enough to keep the response below the threshold φ_{thr} in the absence of noise. Here A^0 is equal to 0.012. With the internal noise $\xi^t_{n,m}$ the threshold φ_{thr} is sometimes crossed at some site and a burst results from this event (Figure 2 (a)). The bursting is longer with larger coupling strength ζ. Given $\zeta = 0.8$ for the present work, the burst duration is about 10 time steps. In the wake of the burst a prolonged suppressed pause lasting about 60 time steps takes place. During this pause susceptibility of lattice sites to noise shocks is suppressed.

Bursts trigger traveling waves that propagate throughout the lattice until they pass away on the lattice boundary or are annihilated by virtue of wave collision. These waves are mostly target types (Figure 2, b and c). Their lifetime, beginning with the burst triggering and ending with disappearing on the lattice boundary, is about 100 time steps. Spiral waves [30, 31] can occasionally emerge as well, predominantly at large noise intensities (Figure 2, d and e). Revolution of the spiral waves takes around 90 time steps. They occupy the lattice space *via* rotation of their arms and hamper the noise creation of new bursts.

3. Phase transition with respect to the parameter σ

Lattice response is represented through variables [31]

$$Z^t_{n,m} = \frac{1}{2}(\varphi^t_{n,m} + \varrho^t_{n,m}), \qquad J^t_{n,m} = \frac{1}{2}(\varphi^t_{n,m} - \varrho^t_{n,m}), \tag{11}$$

projected on the plane (Z, J) for a visual representation. Figure 3 demonstrates a snapshot of a typical suprathreshold response projected onto the plane (Z, J) at the instant a traveling wave occupies a wide lattice space.

A box with maximum permissible sizes $B = \{(Z_{\min}, Z_{\max}), (J_{\min}, J_{\max})\}$ covering the given area is called the *support* [8] of the variable set $\{Z^t_{n,m}, J^t_{n,m}\}$. Let an array

$$R = \text{array}[i = 1..192,\ j = 1..256] \tag{12}$$

be a finite partition [2] of the support B. This array divides the support into 192×256 cells [31] with finite dimensions $\Delta Z = (Z_{\max} - Z_{\min})/192$, $\Delta J = (J_{\max} - J_{\min})/256$ each. The variable set $\{Z^t_{n,m}, J^t_{n,m}\}$ induces in the sample set R at every instant t a dynamic distribution density $\rho_{i,j}[t]$ [2]

$$\sum_{i,j} \rho_{i,j}[t] = 1, \tag{13}$$

where the summation runs over the sample set R of equation (12).

The time-averaged Shannon entropy from this sample set is

$$S = -\lim_{T\to\infty} \frac{1}{T} \sum_{t=1}^{T} \sum_{i,j} \rho_{i,j}[t] \ln[\rho_{i,j}[t]]. \tag{14}$$

Figure 4 shows the entropy calculated in the absence of an external signal for various values of the noise amplitude σ. Two regions, 1 and 2, are seen wherein two different laws of entropy are followed; namely, in region 1

$$S_1 = a_1 + \ln[\sigma], \tag{15}$$

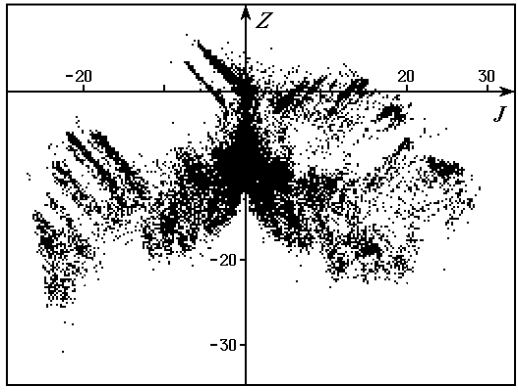

Figure 3. Snapshot of a suprathreshold response of the CML from equation (1) projected onto the plane (Z, J). The lattice parameters are the same as in Figure 2. The support $\{(Z_{\min}, Z_{\max}), (J_{\min}, J_{\max})\}$ is closed to $\{(-36.0,\ 13.0), (-29.0,\ 33.0)\}$.

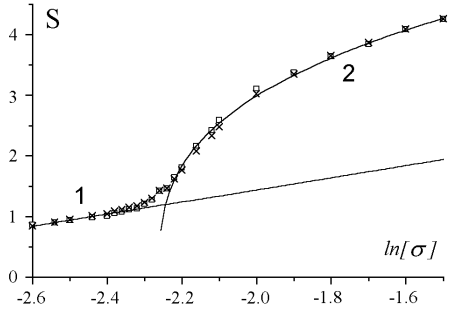

Figure 4. Phase transition seen as breakdown of entropy behavior in the vicinity of the point $\ln[\sigma] \approx -2.24$. Magnitudes of the entropy from equation (14) and the quantity of equation (17) are depicted by open squares and crosses, respectively.

and in region 2

$$S_2 = a_2 \left(\frac{\ln[\sigma_*] - \ln[\sigma]}{\ln[\sigma_*]} \right)^{0.333}, \tag{16}$$

are disclosed. They are traced by solid lines at the fitted parameters $a_1 \approx 3.44$, $a_2 \approx 6.14$, and $\ln[\sigma_*] \approx -2.26$. Intersection of the relations S_1 and S_2 determines the phase transition point $\ln[\sigma_c] \approx -2.243 \mapsto \sigma_c \approx 0.106$.

In the same figure the relation

$$S_\times = S_1 + a_3 K_{\mathrm{ZJ}} \tag{17}$$

is depicted by crosses. Here support S_1 is the linear relation of equation (15), the term

$$K_{\mathrm{ZJ}} = \lim_{T\to\infty} \frac{1}{T} \sum_{t=1}^{T} \frac{1}{N^2} \sum_{n,m} Z^t_{n,m} J^t_{n,m} \tag{18}$$

is the time-averaged functional [31] represented by the scalar product of two system state vectors $\vec{\mathbf{Z}}[t] = \{Z^t_{n,m}\}$ and $\vec{\mathbf{J}}[t] = \{J^t_{n,m}\}$, and the fitted parameter $a_3 \approx 2.1$. The scalar product of these vectors represents, with an accuracy of factor, an entropy production [31]. Since the system resides, predominantly for region 1, in the basin of the point attractor $Z = J = 0$, the entropy production in region 1 is equal to zero [29]. One can see that K_{ZJ} is close to zero in this region as well. S_1 from equation (15) is solely responsible for the entropy increment in this region due to the productive function of the noise source equation (9). The quantity K_{ZJ} becomes nonzero in region 2. Here traveling waves are continuously sustained by the noise source [19]. The quantity K_{ZJ} is seen to be an order parameter for this transition.

4. Stochastic resonance

Examination of system response to external perturbation gives important information about processes that take place in the vicinity of the phase transition point. The perturbation used in the present work is a small periodic signal $A^0_{n,m} \cos[\Omega \cdot t]$. Examination of system response in this fashion is essentially associated with SR investigation in the CML [32].

Residence time distribution is an important characteristic of SR [12, 17]. Let us first examine the residence time of equation (1) in the subthreshold state, $\varphi^t_{n,m} < \varphi_{\mathrm{thr}}$ for all n and m at the same time; that is, the residence time in the basin of the point attractor. Figure 5 shows different residence time distribution histograms $N[T]$ for selected noise amplitudes σ and an external signal with the driving period $T_\Omega = 2\pi/\Omega = 240$. Peaks seen in the lower histogram are centered at multiples $T/T_\Omega = (2n-1)/2$, $n = 1, 2, \ldots$. The height of the first peak $P_{n=1}$ characterizes selective response of the system to the external signal [12], as illustrated in the inset. As can be seen, there is an optimal range of the noise amplitude ($-2.5 < \ln[\sigma] < -2.1$) where system selective response to the external signal increases due to the noise influence.

The responses to external signals for several periods $T_\Omega = 120$, 240, and 480, manifesting themselves by passage of the first peak P_1 over the maximum apex as σ passes along the optimal noise range, are shown in the left column in Figure 6. The right column in Figure 6 presents the Shannon entropy (equation (14)) calculated at the same conditions

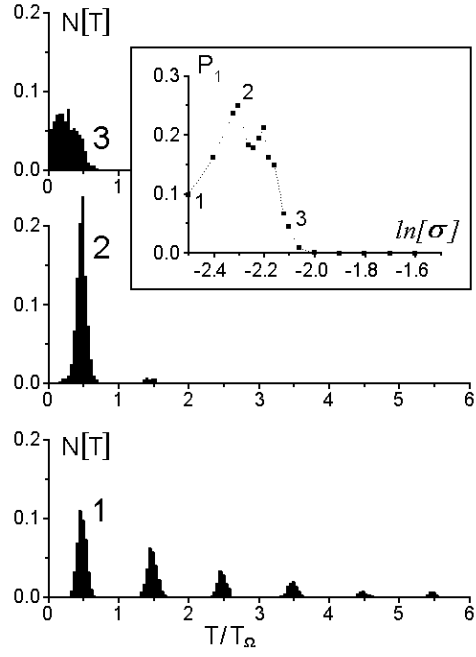

Figure 5. Residence time distribution histogram $N[T]$ for various noise amplitudes σ and fixed parameters of the driving input ($A^0 = 0.012$, $T_\Omega = 240$). Inset shows height of the first peak P_1 of $N[T]$ *versus* $\ln[\sigma]$. The numbers 1, 2, and 3 (in both figures and inset) correspond to $\ln[\sigma]$ values of -2.5, -2.3, and -2.1, respectively.

(depicted by open squares). Solid lines depict equations (15) and (16) representing a background for the entropy calculated in the presence of the external signal. Against this background the entropy increment is clearly visible in the transition region. The quantities $S_\times$ undergo similar increments as well, through increments of K_{ZJ} from equation (15). They are depicted by crosses in this figure. Excesses of these quantities, $\Delta S = S - \widetilde{S}$ and $\Delta K = K_{\mathrm{ZJ}} - \widetilde{K}_{\mathrm{ZJ}}$, with respect to the background $\widetilde{S}$ and $\widetilde{K}_{\mathrm{ZJ}}$ (see Figure 4) refer to the information capacity [24] of the SR. These excesses for different periods T_Ω are shown in Figure 7. Apexes of these excesses can be seen arranged in the vicinity of the phase transition point $\ln[\sigma_c] \approx -2.243$. The maximum apex, in so doing, is at $T_\Omega \simeq 160 \div 180$. Thereafter, the height of the apex decreases smoothly as T_Ω increases. In fact, enhancement of SR taking place near $T_\Omega \approx 160$ is induced by coincidence of the external signal frequency with the internal rhythm of the system, that is, the resonance relation $T_\Omega \doteq 2\,T$ is valid for traveling waves, the lifetime of which is $T \approx 80$.

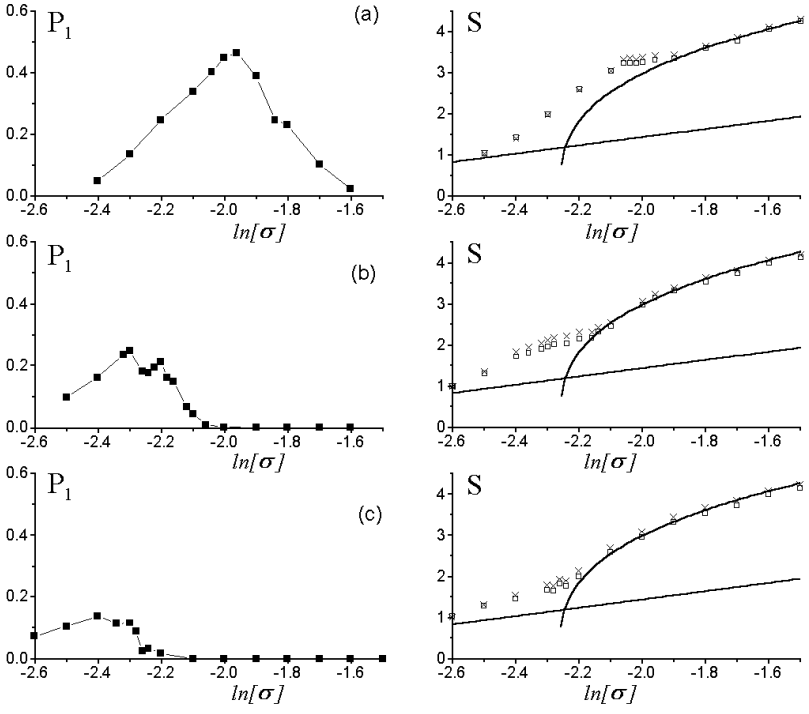

Figure 6. SR phenomenon with respect to σ. The left column shows the height of the first peak P_1 of the residence time histogram $N[T]$. The right column shows the Shannon entropy from equation (14) and the quantity of equation (17) (depicted by open squares and crosses, respectively) calculated with various driving periods T_Ω for the external signal: (a) $T_\Omega = 120$; (b) $T_\Omega = 240$; (c) $T_\Omega = 480$. The lines in the right-hand graphs are drawn according to equations (15) and (16).

5. Conclusions

The noise induced phase transition studied in the two-dimensional coupled map lattice (CML) of equation (1) is a transition from sporadic suprathreshold excursions provoked by small noise intensity to noise enhanced traveling waves as the noise intensity becomes large enough. The Shannon entropy and entropy production are shown to undergo qualitative changes in the phase transition point with respect to the noise intensity. Susceptibility of the system to an external subthreshold perturbation increases enormously in the vicinity of this point. The phase transition region is a region where stochastic resonance (SR) can be realized due to an increasing susceptibility to external subthreshold signals. SR manifests itself in phase locking [27] between the periodic

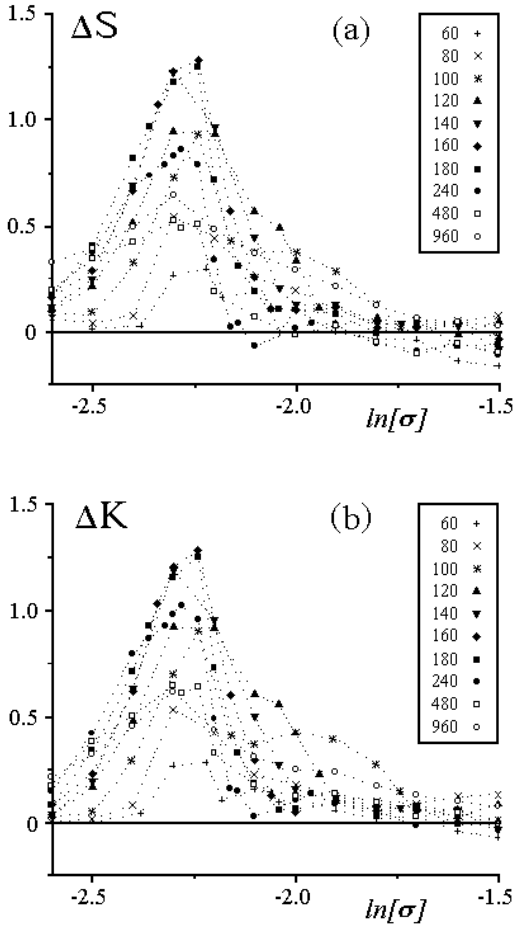

Figure 7. SR complexity emerging in the transition region. Families of excesses ΔS (a) and ΔK (b) are shown for various T_Ω = 60, 80, 100, 120, 140, 160, 180, as well as for 240, 480, and 960.

drive added in the central part of the lattice and lattice site burstings that trigger the traveling waves.

Detection of events near the threshold of perception and, possibly, below it, for disclosing a danger or finding food in time of scarcity, is essential for the survival of living beings in the environment. For this reason, SR can play a significant role for signal transmission in neural information processing [22, 25, 26]. SR was recently demonstrated by Gluckman and others [13] in slices of the rat hippocampal. It is known from experience that the hippocampus is a structure that has a low seizure threshold [14]. In essence, this structure acts on the edge of loss

of stability and epileptic seizures can be readily provoked there [7, 18, 33]. As a consequence, its perceptibility of external signals in this active region is high enough.

Acknowledgments

The author gratefully acknowledges M. A. Pustovoit for useful discussions and valuable remarks. The author also thanks V. V. Deriglazov for fruitful discussions about the phase transition phenomena. This work was supported by the Russian Foundation for Basic Research under grant Number 97–01–01078.

References

[1] D. V. Arnold, "Information-theoretic Analysis of Phase Transition," *Complex Systems*, **10** (1996) 143–155.

[2] C. Beck and F. Schlögl, *Thermodynamics of Chaotic Systems* (Cambridge University Press, Cambridge, 1993).

[3] M. C. Cross and P. C. Hohenberg, "Pattern Formation Outside of Equilibrium," *Reviews of Modern Physics*, **65** (1993) 851–1112.

[4] K. R. Crounse, L. O. Chua, P. Thiran, and G. Setti, "Characterization and Dynamics of Pattern Formation in Cellular Neural Networks," *International Journal of Bifurcation and Chaos,* **6** (1996) 1703–1724.

[5] J. P. Crutchfield and K. Young, "Inferring Statistical Complexity," *Physical Review Letters*, **63** (1989) 105–109.

[6] R. Dogaru and L. O. Chua, "CNN Genes for One-dimensional Cellular Automata: A Multi-nested Piecewise-linear Approach," *International Journal of Bifurcation and Chaos*, **8** (1998) 1987–2001.

[7] A. O. Dudkin and V. I. Sbitnev, "Coupled Map Lattice Simulation of Epileptogenesis in Hippocampal Slices," *Biological Cybernetics*, **78** (1998) 479–486.

[8] J.-P. Eckmann and D. Ruelle, "Ergodic Theory of Chaos and Strange Attractors," *Reviews of Modern Physics*, **57** (1985) 617–656.

[9] R. F. Fox, "Second-order Algorithm for the Numerical Integration of Colored-noise Problems," *Physical Review A*, **43** (1991) 2649–2654.

[10] T. D. Frank, A. Daffertshofer, P. J. Beek, and H. Haken, "Impacts of Noise on a Field Theoretical Model of the Human Brain," *Physica D*, **127** (1999) 233–249.

[11] W. J. Freeman "Nonlinear Gain Mediating Cortical Stimulus–Response Relations," *Biological Cybernetics*, **33** (1979) 237–247.

[12] L. Gammaitoni, P. Hänggi, P. Jung, and F. Marchesoni, "Stochastic Resonance," *Reviews of Modern Physics*, **70** (1998) 223–287.

[13] B. J. Gluckman, T. I. Netoff, E. J. Neel, W. L. Ditto, M. L. Spano, and S. J. Schiff, "Stochastic Resonance in a Neuronal Network from Mammalian Brain," *Physical Review Letters*, **77** (1996) 4098–4101.

[14] J. D. Green, "The Hippocampus," *Physiological Reviews*, **44** (1969) 561–608.

[15] H. Haken, "Pattern Formation and Pattern Recognition—An Attempt at a Synthesis," in *Pattern Formation by Dynamic Systems and Pattern Recognition* (Proceedings of the International Symposium on Synergetics), edited by H. Haken, (Springer-Verlag; Berlin, Heidelberg, and New York, 1979).

[16] H. Haken, *Synergetics—An Inroduction: Nonequilibrium Phase Transitions and Self-organization in Physics, Chemistry, and Biology*, (Springer-Verlag; Berlin, Heidelberg, and New York, 1983).

[17] S. M. Hess and A. M. Albano, "Minimum Requirements for Stochastic Resonance in Threshold Systems," *International Journal of Bifurcation and Chaos*, **8** (1998) 395–400.

[18] M. S. Jensen and Y. Yaari, "Role of Intrinsic Burst Firing, Potassium Accumulation, and Electrical Coupling in the Elevated Potassium Model of Hippocampal Epilepsy," *Journal of Neurophysiology*, **77** (1997) 1224–1233.

[19] P. Jung, "Thermal Waves, Criticality, and Self-organization in Excitable Media," *Physical Review Letters*, **78** (1997) 1723–1726.

[20] P. Jung and G. Mayer-Kress, "Noise Controlled Spiral Growth in Excitable Media," *International Journal of Bifurcation and Chaos*, **5** (1995) 458–462.

[21] P. Jung and G. Mayer-Kress, "Spatiotemporal Stochastic Resonance in Excitable Media," *Physical Review Letters*, **74** (1995) 2130–2133.

[22] S. Kádár, J. Wang, and K. Showalter, "Noise-supported Travelling Waves in Sub-excitable Media," *Nature (London)*, **391** (1998) 770–772.

[23] D. E. Knuth, *The Art of Computer Programming* (Addison-Wesley, Reading, MA, 1969).

[24] C. G. Langton, "Computation at the Edge of Chaos," *Physica D*, **42** (1990) 12–37.

[25] J. F. Lindner, S. Chandramouli, A. R. Bulsara, M. Löcher, and W. L. Ditto, "Noise Enhanced Propagation," *Physical Review Letters*, **81** (1998) 5048–5051.

[26] M. Löcher, D. Cigna, and E. R. Hunt, "Noise Sustained Propagation of a Signal in Coupled Bistable Electronic Elements," *Physical Review Letters*, **80** (1998) 5212–5215.

[27] A. Neiman, A. Silchenko, V. Anishchenko, and L. Schimansky-Geier, "Stochastic Resonance: Noise-enhanced Phase Coherence," *Physical Review E*, **58** (1998) 7118–7125.

[28] Y. Pomeau and P. Manneville, "Intermittent Transition to Turbulence in Dissipative Dynamical Systems," *Communications in Mathematical Physics*, **74** (1980) 189.

[29] I. Prigogine, *From Being to Becoming: Time and Complexity in the Physical Sciences* (W. H. Freeman and Company, San Francisco, 1980).

[30] V. I. Sbitnev, "Checkerboard Spiral Waves in a 2D Coupled Map Lattice," *International Journal of Bifurcation and Chaos*, **7** (1997) 2569–2575.

[31] V. I. Sbitnev, "Chaos Structure and Spiral Wave Self-organization in 2D Coupled Map Lattice," *International Journal of Bifurcation and Chaos*, **8** (1998) 2341–2352.

[32] V. I. Sbitnev and M. A. Pustovoit, "Stochastic Resonance in 2D Coupled Map Lattice Model of Field-like Neural Tissue," *International Journal of Bifurcation and Chaos*, (submitted to press).

[33] K. L. Smith, C. L. Lee, and J. W. Swann, "Local Circuit Abnormalities in Chronically Epileptic Rats After Intrahippocampal Tetanus Toxin Injection in Infancy," *Journal of Neurophysiology*, **79** (1998) 106–116.

[34] S. Wolfram, "Universality and Complexity in Cellular Automata," *Physica D*, **10** (1984) 1–35.

[35] T. Yang and L. O. Chua, "Control of Chaos Using Sampled-data Feedback Control," *International Journal of Bifurcation and Chaos*, **8** (1998) 2433–2438.